Urol Res (2005) 33: 213–219
DOI 10.1007/s00240-004-0456-0

ORIGINAL PAPER

Jennifer Anderson · Jessica Dellomo
André Sommer · Andrew Evan · Sharon Bledsoe

A concerted protocol for the analysis of mineral deposits in biopsied tissue using infrared microanalysis

Received: 4 June 2004 / Accepted: 25 October 2004 / Published online: 10 February 2005

Abstract The mechanism(s) by which crystals are retained in the kidney resulting in stone disease remains unclear. Intratubular aggregation as well as crystal cell binding, or internalization and translocation, or alternatively nucleation and growth in the interstitial fluid are possible models. Our group is testing the hypothesis that calcium phosphate deposits in kidneys of patients with calcium renal stones arise in unique anatomical regions of the kidney. Furthermore, we believe that their formation is conditioned by specific stone forming pathophysiologies. To test this hypothesis, we performed intra-operative renal papillary biopsies during percutaneous nephrolithotomy of kidneys from 15 idiopathic calcium stone formers as well as kidney tissue from a patient who ingested ethylene glycol, and developed a new protocol to accurately identify the composition of the calcium deposits located in the renal tissue. We developed a new histological approach that incorporated a low-energy (low-E) reflective slide substrate that has similar characteristics to a common microscope slide and infrared absorption microspectroscopy. Infrared absorption microspectroscopy revealed the crystal deposits in the idiopathic calcium oxalate stone formers to be hydroxyapatite in composition with an occasional region of calcium carbonate, while calcium oxalate was the predominant mineral in the kidney of the patient who had ingested ethylene glycol. The results demonstrate that mixed sample types containing tissue and mineralized deposits are easily analyzed while mounted on a low-E slide using the attenuated total internal reflectance (ATR) method. Reflection/absorption (R/A) analysis allows one to quickly survey a tissue section and provides qualitative information about its components. Once interesting sites have been identified by R/A analysis, ATR analysis can then be used to collect the best data possible. ATR analysis provides spectra free from many of the artifacts associated with transmission and R/A analysis, and completes the full picture of the components contained in the crystal deposits and tissue. We present a method of analysis for mineralized materials embedded in kidney tissue that uses readily or easily obtainable materials and instrumentation. The sensitivity of this method allows tissue sections to remain unstained, alleviating the tedious and time-consuming constraints of earlier methods of visual analysis. The present method will save time and training, while simultaneously offering an unbiased analysis of mineralized components that is more accurate and conducive to patient treatments than previous methods.

Keywords Infrared microspectroscopy · Mineral deposits · Renal stones · Tissue biopsy · Reflection/absorption · Imaging

Introduction

For well over 160 years, disease detection in biopsied tissue has relied on the painstaking preparation of thin sections followed by contrast staining to visibly signal the presence or absence of disease. For most tissue biopsies, thin sectioning and contrast staining procedures are considered routine. The identification of crystals in renal biopsies has relied on the visual inspection of the morphology of a crystal using a light microscope and/or employing selective staining protocols to take advantage of the mineral properties of a particular crystal. Such approaches are subject to investigator bias and skill level.

Infrared and x-ray diffraction methodologies have been successfully used on isolated renal calculi because

---

J. Anderson · J. Dellomo · A. Sommer (✉)
Molecular Microspectroscopy Laboratory,
Department of Chemistry and Biochemistry,
Miami University, Oxford, OH 45056 USA

A. Evan · S. Bledsoe
Department of Anatomy and Cell Biology,
Indiana University School of Medicine,
Indiana University—Purdue University Indianapolis,
Indianapolis, IN 46202 USA

of their ability to yield highly accurate spectra of mineral composition [1, 2, 3, 4, 5, 6, 7, 8, 9, 10, 11, 12, 13, 14, 15, 16, 17, 18, 19, 20, 21, 22]. However, the problem with these previous studies is that they analyzed macroscopic sized samples of mineral and not the micron-sized crystalline deposits we are interested in identifying in the kidney tissue of stone formers [23]. The integration of a microscope to the infrared spectrometer allows the infrared beam to be focused in microscopic crystal domains at specific areas of a larger sample. This approach is termed infrared absorption microspectroscopic imaging and provides a unique molecular fingerprint of the crystalline deposits to be studied. This technique has been previously employed on tissue sections with very positive results [6, 15, 16, 17, 18, 19, 20, 21, 22, 24]. However, unlike the research presented here, the samples analyzed in these studies did not contain minerals embedded in the tissue. In addition, the previous tissue samples had been stained and held between two infrared-transparent windows, while here, they have the option of remaining unstained and merely mounted onto a reflective glass substrate.

Our laboratory has been interested in determining the pathogenesis of the most common form of human kidney stones: idiopathic calcium oxalate stone disease. In order to determine the mechanisms responsible for the formation of these stones, we are required to be able to accurately characterize the mineral composition of very small crystalline deposits located within the tissue compartments of these kidneys. Thus, the goal of this study was to develop a new histological approach that incorporated a low-energy (low-E) reflective slide substrate that has similar characteristics to a common microscope slide, and infrared absorption microspectroscopy to accurately determine the mineral composition of these small crystals. The initial step in this new protocol allows the histologist to prepare tissue sections in the traditional manner, but then mount the tissue on the reflective slide. This same reflective slide is employed for visible as well as infrared analysis of a single tissue section. When combined with infrared analysis, this protocol allows fast and easy examination of mixed samples, omitting the process of staining tissue samples while allowing the analysis and identification of both tissue and embedded crystal deposits. Both reflection/absorption (R/A) as well as attenuated total internal reflection (ATR) analysis of the tissue and embedded material can be performed on the low-E substrate, yielding qualitative, unbiased and accurate information about the mineralized stone components and the embedding tissue media.

Materials and methods

Tissue biopsy samples were obtained from the Indiana University Medical School with the informed consent of the patients, and were prepared by a certified histologist. The patients varied in age, symptoms and backgrounds, and are described in our recent study [23]. The unstained tissue sections on the low-E substrates were imaged using the visible CCD camera and frame grabber on the Spectrum Spotlight. A serial section stained with Yasue silver replacement stain was employed as a control to confirm the location of the calcium [25]. This serial section was reviewed using a standard visible microscope in an attempt to visually determine the general area of the mineralized crystals of interest.

Tissue sections from 15 patients with idiopathic calcium oxalate kidney stone disease and an individual who ingested ethylene glycol, as well as cross-sections of unembedded calculi were analyzed in the present study. Papillary biopsies were obtained at the time of percutaneous nephrolithotomy from a group of 15 well-characterized idiopathic calcium oxalate stone formers. In addition, renal biopsies were collected from four control kidneys at the time of surgical removal of upper urinary tract cancer while large tissue samples were obtained at the time of autopsy from one patient who died from ethylene glycol ingestion.

All samples were analyzed by a Perkin-Elmer Spectrum Spotlight 300 infrared imaging microscope that was equipped with an array detector for the rapid acquisition of molecular images and a single point detector for the acquisition of high signal to noise spectra with a lower wavenumber cutoff of 580 cm^{-1}. Both detectors were based on the well-established mercury cadmium telluride (MCT) technology. The minimum sample size that can be analyzed using either detector was approximately two wavelengths (ca. 6 μm). The majority of spectra presented in this report were collected using the single point detector and represent the average of 64 individual scans collected at a spectral resolution of 4 cm^{-1}. The microscope can be operated in transmission, reflection or attenuated total internal reflection (ATR) modes. In the latter mode, a drop-down Ge internal reflection element (IRE) was employed. A 50×50 μm confocal aperture was employed to isolate the sample region of interest for the transmission and reflection modes. The same aperture was employed for the ATR mode, however, the Ge IRE provides an additional 4× magnification resulting in a sampling area of ~13×13 μm.

The substrate used in this investigation was a low-E glass slide (Kevley Technologies, Chesterland, Ohio) [26]. The slides have the same dimensions as those of standard glass microscope slides, making the mounting of tissue samples routine for histologists.

Results

Early procedures to determine an infrared microspectroscopic technique for inclusion determination revolved around transmission analysis. Figure 1 displays both a visible image and a false-color infrared image of a 4 μm

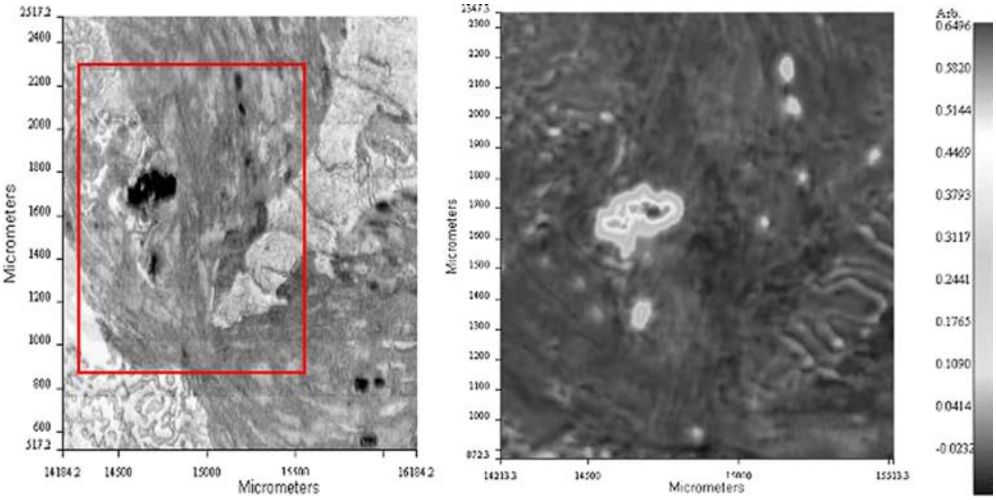

Fig. 1 Visible image (*left*) and an IR transmission false-color image (*right*) of a 4 µm-thick tissue section with a renal stone inclusion between two BaF_2 discs

thick tissue section containing an interstitial mineral deposit that has been embedded in paraffin and compressed between two BaF_2 windows. The patient was diagnosed as an idiopathic calcium oxalate stone former, although currently, infrared analysis classifies the mineralized deposits within the kidney to be calcium phosphate, specifically, hydroxyapatite.

Transmission spectra were collected from the boxed area on the visible image in Fig. 1 to produce the false-color infrared image. The false-color image is made up of approximately 4,000 spectra, which were collected in parallel during a 15-min experiment. This image is based on the peak height of the asymmetric stretching vibration (1,050 cm^{-1}) of the orthophosphate group associated with hydroxyapatite. The image exemplifies the benefit of infrared imaging for the study of tissue. In addition to eliminating the staining procedure, interpretation of the results is much less subjective than current methods of crystal deposit identification.

In the context of the present study, mineral deposits present a problem in that they absorb strongly and scatter infrared radiation, which ultimately affects the results and potential quantitative capacity of the method. Figure 2 illustrates the transmission spectra of a crystal located within a kidney section (top) and of the tissue only (bottom) extracted from the infrared image in Fig. 1. The spectrum of the tissue is photometrically accurate, whereas that of the crystal is not. The feature (1,050 cm^{-1}) associated with the hydroxyapatite is totally absorbing, exhibiting percent transmission values that approach zero. In addition, the entire spectrum has a positive sloping baseline going toward lower wavenumbers. These artifacts arise from the strong absorbance of the deposit and the propensity for scattering, respectively. As the size of the crystal decreases, scattering becomes more problematic, which could make identification difficult. Strong negative transmission bands can be noticed in the spectra of Fig. 2 for both the

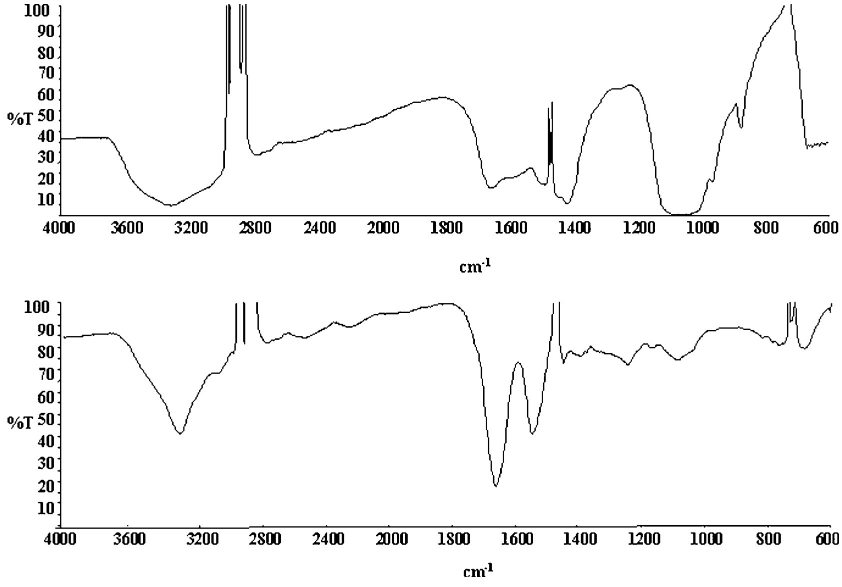

Fig. 2 Transmission spectra of both tissue (*bottom*) and calculus (*top*) from an embedded sample

crystal and tissue near 2,900 and 1,450 cm^{-1}. These features are due to uncompensated embedding (paraffin) material. The embedding material is a hydrocarbon, which absorbs near 2,900, 1,450 and 720 cm^{-1}.

Subsequent to transmission analysis, stained samples containing inclusions were mounted on low-E slides for R/A analysis. Figure 3 illustrates the visible image of a stained tissue sample from the patient who ingested ethylene glycol. Fig. 4 illustrates infrared spectra obtained on a stained mineral deposit using R/A combined with ATR sampling modes. Based on infrared features observed in the R/A spectrum, it appears as though the deposit is comprised mostly of tissue. Again, the sloping baseline indicates the presence of scattering. The most prominent features in the infrared spectrum are the N-H asymmetric stretch and the amide I and amide II bands located at 3250, 1650 and 1550 cm^{-1}, respectively. All of these features are characteristic of protein. Upon closer inspection, the spectrum reveals an inverted absorption located near 780 cm^{-1}. This feature is present in all R/A spectra of the deposits collected from this particular series of samples, and is absent in spectra of the tissue. The patient was diagnosed with ethylene glycol poisoning and oxalate crystals in the kidney tubules; since calcium oxalate has a feature near the absorption in question, the presence of the inverted band was employed as evidence for the presence of calcium oxalate. The negative absorption (Reststrahlen band) arises from anomalous dispersion, which is caused by increased Fresnel reflection near strong absorption bands. The spectrum demonstrates that R/A is a viable method in this particular cases.

Discussion

Initial attempts to study the tissue sections involved the use of transmission infrared microspectroscopy due to the fact that this method typically yields the best results when the long-term goal includes quantitative analysis. However, this mode requires extensive sample preparation to ensure that the sample thickness is on the order of 2–6 μm. This thickness yields infrared spectra of proteinaceous materials in which the minimum transmittance is no less than 20%, a requirement for quantitative analysis and photometrically accurate band intensities. Further, the sample must be mounted flat on an infrared transparent window in order to avoid sloping baselines or artifacts in the spectrum. Most transmission analysis of tissue samples involves mounting a wet or dry section between two barium fluoride (or similar) windows [6, 15, 17, 18, 19, 20, 22, 24], which are transparent from 50,000 cm^{-1} down to 750 cm^{-1} [27]. Barium fluoride is hard and non-hygroscopic, unlike alkali halide windows such as NaCl or KBr. Mounting the tissue between two windows in a low compression cell ensures that the sample remains relatively flat over an area of approximately 1 cm^2.

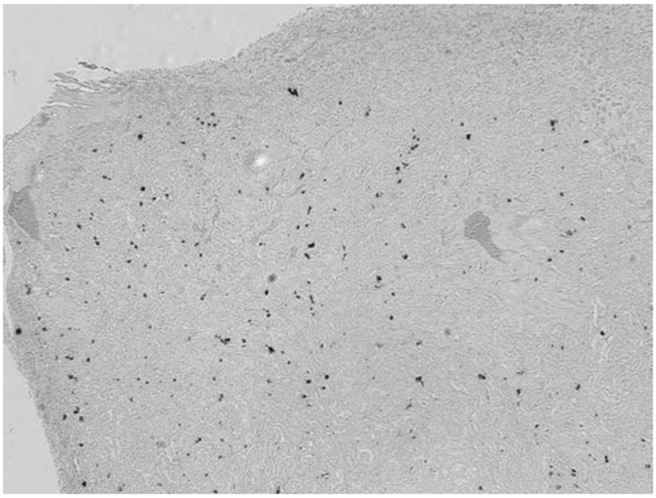

Fig. 3 Visible image of a Yasue-stained tissue section mounted upon a low-E slide from an individual who ingested ethylene glycol. Many oxalate crystals were embedded in the tissue

The major drawback to the transmission mode of analysis is the extensive sample preparation and the introduction of substrate materials that are considered foreign to the histologist. In order for a technique to be quickly accepted by the medical community, it should employ methods that are commonly practiced in that community. In addition, barium fluoride windows are expensive, somewhat brittle, and are commonly furnished as round disks with a diameter of 13 mm and a thickness of 2 mm. Although micro-arrays of tissue sections deposited on barium fluoride have been developed [28, 29, 30, 31, 32, 33], they can be very costly and time consuming to prepare. Finally, barium fluoride is only transparent down to 750 cm^{-1}. The region below 750 cm^{-1} is sometimes useful for further differentiation of mineralized deposit components.

Following the analysis of tissue sections using a transmission process, reflection/absorption measurements were conducted using the low-E substrate [26]. These slides have similar physical characteristics to conventional glass microscope slides with the exception of a thin three-layer reflective coating on the surface of one side. Tissue analysis using low-E slides has been performed previously with much success [34].

The homogeneity of the low-E substrate was tested by spin coating a thin film (approximately 0.6 μm) of poly(methylmethacrylate) on the surface of the substrate. Six slides, taken from two different batches produced by the manufacturer, were coated with the resultant films exhibiting a faint purple hue. The peak area of the carbonyl (C=O) absorption from 125 infrared spectra in each map collected over a ~4.0×4.0 mm^2 area for each slide was determined. The average relative standard deviation of the peak area was less than 10.7% over the mapped area. The thickness of spin cast films is known to vary by ~10% independent of area. The results demonstrate that the reflection properties of the low-E slide are homogeneous over an

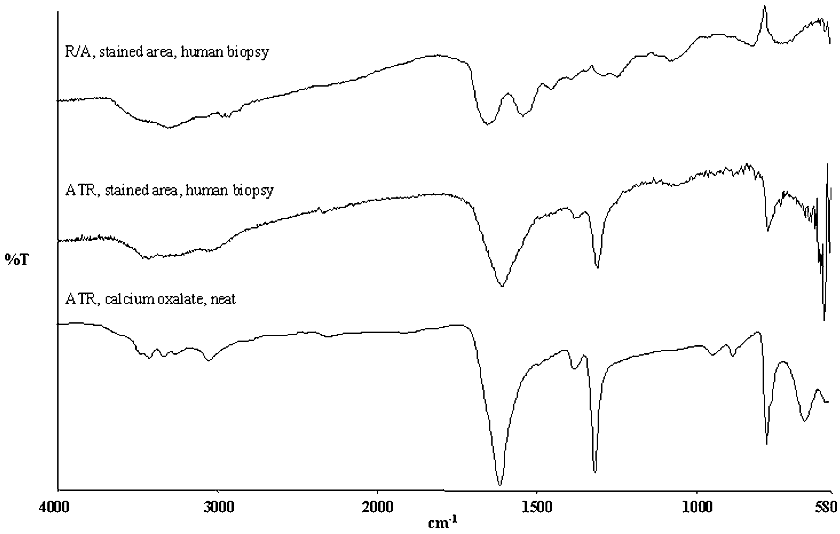

Fig. 4 Spectra of calcium oxalate in human biopsy. R/A (*top*), ATR (*middle*), and calcium oxalate ATR standard (*bottom*)

area of 4.0×4.0 mm^2, which should be sufficient for most histological analyses.

Although the R/A spectrum is useful from a qualitative perspective, quantitative considerations exemplify two shortcomings. First, in the reflectance mode, the optical path length is approximately double that of a transmission mode (see Fig. 5). It is approximately double since the radiation must pass through the sample, reflect from the substrate, and pass back through the sample again before reaching the detector. As such, the thickness of the section should be one-half that required for transmission, should any quantitative analysis be attempted. Second, scattering and reflection artifacts are still present, which could significantly affect the interpretation of results. Finally, the identification of calcium oxalate should be based on more than one feature, even if it is a well-behaved and reproducible one as in the case presented here.

In contrast to the R/A spectrum, Fig. 4 also presents a spectrum obtained on the same mineralized deposit using the ATR method. In this method, a shaped germanium IRE is placed in contact with the sample. The tip of the IRE is ~100 μm, however, the sampled area is dependent upon the refractive index of the IRE and the size of the confocal aperture [35]. For the same aperture size as used in transmission or reflection/absorption analysis, the sampled area is four times smaller in the ATR analysis due to the 4× magnification associated with the refractive index of the germanium IRE. The spectrum obtained on the deposit clearly shows the asymmetric and symmetric stretching modes of the oxalate anion located at 1,620 and 1,318 cm^{-1}, respectively. A reference ATR spectrum of calcium oxalate is provided for comparison. An added benefit of the ATR method is that the penetration of the infrared radiation into the sample is less than 1 μm. Thus, for samples thicker than this penetration depth, the optical path through the sample is independent of sample thickness. As a result, photometrically accurate spectra can be obtained on all the materials associated with renal stones without having to worry about the thickness of the section. The reduced path length also reduces scattering that is not only particle size dependent, but path length dependent as well. The only drawback to the ATR method is that the IRE contacts the sample, which could potentially damage it. However, the quality of the spectrum is, by far, the best of all the methods presented when taking all things into consideration.

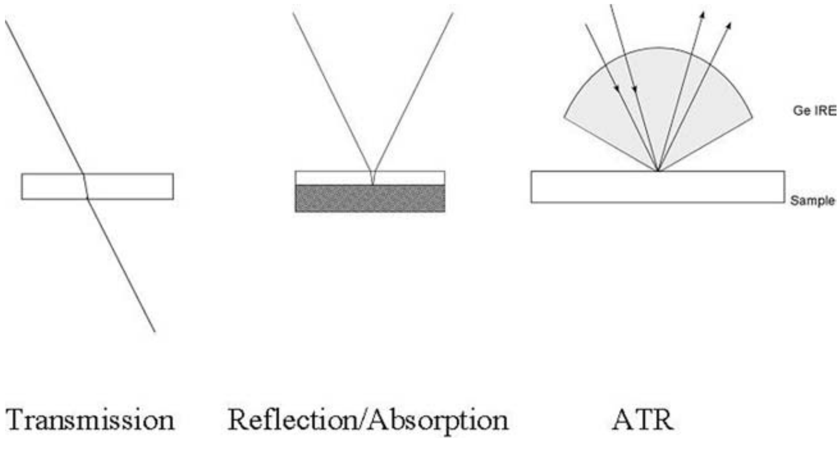

Fig. 5 Transmission, R/A, and ATR diagrams showing the path of light through a sample

The results demonstrate that mixed sample types containing tissue and mineralized deposits are easily analyzed while mounted on a low-E slide using the ATR method. R/A absorption analysis allows one to quickly survey a tissue section and provides qualitative information about its components. Once interesting sites have been identified by R/A analysis, ATR analysis can then be used to collect the best data possible. ATR analysis provides spectra free from many of the artifacts associated with transmission and R/A analysis, and completes the full picture of the components contained in the crystal deposits and tissue. ATR analysis of tissue samples has been presented in the past [7, 36], but we are unaware of embedded mineralized deposits analyzed using this method.

The procedural novelty of this approach to tissue and mineral deposit analysis is the ability to qualitatively, and soon we hope quantitatively, determine the components of crystal deposits without extensive histological preparations or the possible subjectivity of a pathologist. In using a low-E slide, the histologist is presented with a familiar substrate as well as decreased responsibility in that the tissue need not be stained. In addition, the pathologist is relieved of the task of transferring the tissue sample to a substrate complementary to infrared analysis, while simultaneously having the ability to determine mineralized material as well as tissue components.

Conclusions

We have presented a method of analysis for mineralized materials embedded in tissue that uses readily or easily obtainable materials and instrumentation. The sensitivity of this method allows tissue sections to remain unstained, alleviating the tedious and time consuming constraints of earlier methods of visual analysis. The method presented in this article will save time and training, while simultaneously offering an unbiased analysis of mineralized components that is more accurate and conducive to patient treatments than previous methods.

References

1. Huleihel M, Erukhimovitch V, Talyshinsky M, Karpasas M (2002) Spectroscopic characterization of normal primary and malignant cells transformed by retroviruses. Appl Spectrosc 56: 640
2. McIntosh L, Mansfield J, Crowson N, Manstch H, Jackson M (1999) Analysis and interpretation of infrared microscopic maps: visualization and classification of skin components by digital staining and multivariate analysis. Biospectroscopy 5: 265
3. Haka A, Kidder L, Lewis EN (2001) A combined spectroscopic imaging and chemometric approach for automatically partitioning tissue types in human prostate tissue biopsies. Proceedings of SPIE 4259: 47
4. Heise HM (2001) Clinical applications of near- and mid-infrared spectroscopy. In: Gremlich H-U, Yan B (eds) Infrared and Raman spectroscopy of biological materials. Marcel Dekker, New York
5. Kidder L, Haka A, Faustino P, Lester D, Levin I, Lewis EN (1998) Infrared spectroscopic imaging as a tool for pathology. Proceedings of SPIE 3257: 178
6. Chiriboga L, Yee H, Diem M (2000) Infrared spectroscopy of human cells and tissue. part vi: a comparative study of histopathology and infrared microspectroscopy of normal, cirrhotic and cancerous liver tissue. Appl Spectrosc 54: 1
7. Dukor R, Liebman M, Johnson B (1998) A new, non-destructive method for the analysis of clinical samples with FT-IR microspectroscopy. Cell Molec Biol 44: 211
8. Yano K, Ohoshima S, Gotou Y, Kumaido K, Moriguchi L, Katayama H (2000) Direct measurement of human lung cancerous and noncancerous tissues by Fourier transform infrared microscopy: can an infrared microscopy be used as a clinical tool? Anal Biochem 287:218–225
9. Strobel H, Heineman W (1989) Chemical instrumentation: a systematic approach. Wiley-Interscience, New York
10. Corns C (1983) Infrared analysis of renal calculi: a comparison with conventional techniques. Ann Clin Biochem 20: 20
11. Carmona P, Bellanato J, Escolar E (1997) infrared and raman spectroscopy of urinary calculi: a review. Biospectroscopy 3: 331
12. Volmer M, DeVries J, Goldschmidt H (2001) Infrared analysis of urinary calculi by a single reflection accessory and a neural network interpretation algorithm. Clin Chem 47: 1287
13. Lehmann C, McClure G, Smolens I (1988) Identification of renal calculi by computerized infrared spectroscopy. Clin Chim Acta 173: 107
14. Estepa L, Levillain P, Lacour B, Daudon M (1999) Infrared analysis of urinary stones: a trial of automated identification. Clin Chem Lab Med 37: 1043
15. Diem M, Chiriboga L, Lasch P, Pacifico A (2002) IR spectra and IR spectral maps of individual normal and cancerous cells. Biopolymers (Biospectroscopy) 67: 349
16. Diem M, Chiriboga L, Pacifico A, Yee H (2000) Infrared microspectroscopy of cells and tissue: infrared spectra and infrared spectral maps of human tissues. Inst Phys Conf Ser 165: 77
17. Diem M, Chiriboga L, Yee H (2000) Infrared spectroscopy of human cells and tissue. VIII: Strategies for analysis of infrared tissue mapping and applications to liver tissue. Biospectroscopy 57: 282
18. Aparicio S, Doty B, Camacho N, Paschalis E, Spevak L, Mendelsohn R, Boskey A (2002) Optimal methods for processing mineralized tissues for fourier transform infrared microspectroscopy. Calcif Tissue Int 70: 422
19. Mendelsohn R, Chen H-C, Rerek M, Moore D (2003) Infrared microspectroscopic imaging maps the spatial distribution of exogenous molecules in skin. J Biomed Optics 8: 185
20. Marcott C, Reeder R, Paschalis E, Boskey A, Mendelsohn R (1999) Infrared microspectroscopic imaging of biomineralized tissues using a mercury-cadmium-telluride focal-plane array detector. Phosphorus, Sulfur Silicon 144–146: 417
21. Chiriboga L, Yee H, Diem M (2000) Infrared spectroscopy of human cells and tissues. part vii: ft-ir microspectroscopy of dnase- and rnase-treated normal, cirrhotic, and neoplastic liver tissue. Appl Spectrosc 54: 480
22. Ouyang H, Sherman P, Paschalis E, Boskey A, Mendelsohn R (2004) Fourier transform infrared microscopic imaging: effects of estrogen and estrogen deficiency on fracture healing in rat femurs. Appl Spectrosc 58: 1
23. Evan A, Lingeman J, Coe F, Parks J, Bledsoe S, Shao Y, Sommer A, Paterson R, Kuo R, Grynpas M (2003) Randall's plaque of patients with nephrolithiasis begins in basement membranes of thin loops of Henle. J Clin Invest 111: 607
24. Diem M, Boydston-White S, Chiriboga L (1999) Infrared spectroscopy of cells and tissues: shining light onto a novel subject. Appl Spectrosc 53: 148A

25. Yasue T (1969) Histochemical identification of calcium oxalate. Acta Histochem Cytochem 2: 83
26. Cohen J, Virnelson C (1992) FT-IR spectrometer window and method, in USPTO, US, Tremco Incorporated, 1992, US Patent 5,160,826
27. Bruker Optics Guide for Infrared Spectroscopy. Bruker Optics, Billerica
28. Bubendorf L, Nocito A, Moch H, Sauter G (2001) Tissue microarray (TMA) technology: miniaturized pathology archives for high-throughput in situ studies. J Pathol 195: 72
29. Kononen J, Hostetter G, Sauter G, Kallioniemi O-P, Brand K, Trivett M (2003) Tissue microarrays. DNA Microarrays 603–607, 644–645
30. Hedvat C V (2003) Tissue arrays. Expr Profiling Hum Tumors 61–72
31. Zhang X-P, Su D, Cheng Q-H (2003) Advantages and applications of tissue microarray technology on cancer research. Chin J Cancer Res 15: 74
32. Skacel M, Skilton B, Pettay JD, Tubbs RR (2002) Tissue microarrays: a powerful tool for high-throughput analysis of clinical specimens: a review of the method with validation data. Appl Immunohistochem Mol Morphol 10:1–6
33. Rimm DL, Camp RL, Charette LA, Costa J, Olsen DA, Reiss M (2001) Tissue microarray: a new technology for amplification of tissue resources. Cancer J 7: 24
34. Dukor R, Marcott C (2001) Method and system for performing infrared study on a biological sample, in USPTO, US, VYsis, Inc, US Patent 6,274,871 B1
35. Patterson B, Danielson N, Sommer A (2003) Attenuated total internal reflectance infrared microspectroscopy as a detection technique for high-performance liquid chromatography. Anal Chem 75: 1418
36. Dukor RK (1999) Method of identifying cellular types in a biological sample supported on an absorptive substrate by infrared spectroscopy, in USPTO, US, Vysis Inc., 1999, US Patent 5,945,674